Measuring the mixing efficiency in a simple model of stirring: some analytical results and a quantitative study via frequency map analysis

Carletti, Timoteo; Margheri, Alessandro

Published in:
Journal of physics A: Mathematical and general

DOI:
10.1088/0305-4470/39/2/002

Publication date:
2006

Document Version
Early version, also known as pre-print

INSTITUTE OF PHYSICS PUBLISHING JOURNAL OF PHYSICS A: MATHEMATICAL AND GENERAL

J. Phys. A: Math. Gen. **39** (2006) 299–312 doi:10.1088/0305-4470/39/2/002

Measuring the mixing efficiency in a simple model of stirring: some analytical results and a quantitative study via frequency map analysis

Timoteo Carletti[1] **and Alessandro Margheri**[2]

[1] Department of Mathematics, University of Namur, 8 rempart de la Vierge, B-5000 Namur, Belgium
[2] Fac. Ciências de Lisboa and Centro de Matemática e Aplicações Fundamentais, Av. Prof. Gama Pinto 2, 1649-003 Lisboa, Portugal

E-mail: timoteo.carletti@fundp.ac.be and margheri@ptmat.fc.ul.pt

Received 2 March 2005, in final form 24 October 2005
Published 14 December 2005
Online at stacks.iop.org/JPhysA/39/299

Abstract

We prove the existence of invariant curves for a T-periodic Hamiltonian system which models a fluid stirring in a cylindrical tank, when T is small and the assigned stirring protocol is piecewise constant. Furthermore, using the numerical analysis of the fundamental frequency of Laskar, we investigate numerically the break down of invariant curves as T increases and we give a quantitative estimate of the efficiency of the mixing.

PACS numbers: 05.45.Gg, 47.52.+j, 47.11.+j

1. Introduction

In [1] a simplified model has been studied for the stirring, by an agitator, of an ideal fluid in a cylindrical tank. A Lagrangian representation is adopted to describe the motion, which is assumed to be completely two dimensional. The tank thus degenerates to its boundary circle, which has radius R. The agitator is modelled as a point vortex of strength Γ and its position inside the boundary circle as a function of time, denoted by $z(t)$, is a prescribed T-periodic function called *stirring protocol*. Introducing the complex coordinate $\zeta = x + \mathrm{i}y$, the motion of the fluid is governed by the following non-autonomous T-periodic Hamiltonian system,

$$\dot{\bar{\zeta}} = \frac{\Gamma}{2\pi \mathrm{i}} \frac{|z(t)|^2 - R^2}{(\zeta - z(t))(\zeta \overline{z(t)} - R^2)}, \tag{1}$$

whose corresponding Hamilton function is given by

$$H(t, \zeta) = \frac{\Gamma}{2\pi} \ln \left| \frac{\zeta - z(t)}{\overline{z(t)}\zeta - R^2} \right|. \tag{2}$$

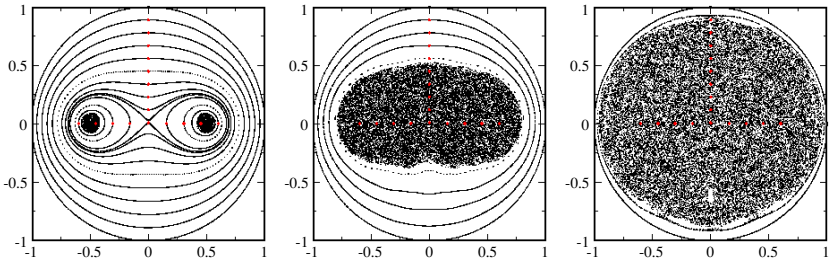

Figure 1. Different behaviours of the Poincaré map, with $b = 1/2$, $R = 1$ and $T = 0.05$ (left), $T = 0.5$ (middle) and $T = 1.5$ (right). Each plot is obtained following 10 000 time units with the same 18 initial data.

(This figure is in colour only in the electronic version)

System (1) is defined on the set $\left\{(t, \zeta) \in \mathbb{R} \times \mathbb{C} : \zeta \neq z(t), \zeta \neq \frac{R^2}{z(t)}\right\}$ and it is considered for ζ belonging to the invariant disc $D_R = \{\zeta \in \mathbb{C} : |\zeta| \leqslant R\}$.

The following piecewise constant stirring protocol,

$$z(t) = \begin{cases} +b & t \in [nT, nT + T/2) \\ -b & t \in [nT + T/2, (n+1)T) \quad n \in \mathbb{Z}, \end{cases} \tag{3}$$

with fixed $0 < b < R$, has been investigated in [1]. In this case the motion can be integrated over finite time, whereas the long time behaviour of the model has been studied with numerical experiments, (most of which) with $b = 1/2$ for different values of T.

In [1], the objective of the author was to study which features control the onset of chaos and hence the efficiency of the mixing. With this aim, the regimes of regular and chaotic behaviour have been identified and a *qualitative* description (see [1], p 736, second paragraph) of the mixing efficiency of the model has been provided for several values of the parameters (b, T). It turns out that the regions of chaotic behaviour consume a larger and larger portion of the phase space as T increases, disrupting the regular pattern observed when T is very small (see figure 1). In particular, we quote [1], "It is clear that as $T \to 0$ the model $[\cdots]$ will look more and more like the two fixed agitator system; $[\cdots]$ Thus one would expect 'convergence' as $T \to 0$." A short remark is presented to support this numerical evidence (namely, for small T the positions of an advected particle may be viewed as coordinates in a 'leapfrog' scheme with step $T/2$ aimed at integrating numerically the two fixed agitators system). In the next section, we will show that averaging theory provides the appropriate framework to investigate the above statement from an analytical point of view. Loosely speaking, we will be able to show that when $T \to 0$ the flow of system (1) with the stirring protocol (3) converges in the C^4 topology to the Hamiltonian flow of the time-averaged system, which corresponds to two fixed agitators. As a consequence, using Moser's small twist theorem [10, 11, 16, 17] we will prove that the regularity of the pattern observed in the numerical experiments for small T (see figures 2(*a*), (*b*) and (*c*) p 733 of [1] and figure 1 for $T = 0.05$) is due, at least in a suitable annular region inside D_R, to the presence of invariant curves. In fact, such curves are, as one readily realizes, an obstruction to the mixing of the fluid.

More precisely, the main result we present is the following:

Theorem 1. *Let $z(t)$ be the stirring protocol (3) and let $T > 0$ be its period. Then, there exists an annular region A inside D_R such that the T-Poincaré map associated with system (1) has invariant curves in A for any sufficiently small T.*

This kind of result is quite standard in perturbation theory. We observe that within this framework other approaches could be used to obtain similar results. For instance, one could look for invariant curves by considering Lindsted series in the small parameters or by using the KAM theorem. We adopt Moser's theorem because its application is simpler, avoiding all the problems with the convergence of series and small divisors.

As T increases the invariant curves break down. In section 3.2, we study numerically this phenomenon by means of the numerical analysis of the fundamental frequency (NAFF) of Laskar [13], a method which we recall in section 3.1. This study allows us to extend our previous analytical result as to cover larger T ranges by showing numerical evidence that invariant curves persist close to the boundary of the invariant disc D_R up to (some) large values of T. Furthermore, in section 3.3 we are able to give a *quantitative* description of the efficiency of the mixing in a function of parameters (b, T) by measuring, through NAFF, the portion of phase space filled by invariant curves.

The NAFF method provides a powerful tool to detect the regularity of a given orbit (see [3, 14], but also [8] where the method is compared with other refined Fourier technics), especially for quasi-integrable Hamiltonian systems in a regime of parameters where the phase space is almost completely foliated by invariant tori [4, 5]. In the opposite situation other methods could be considered, for instance, those which make use of the notion of *maximal Lyapunov exponent* [20], and of *conditional entropy* [4] or the MEGNO method [5]. Nevertheless, we preferred to use NAFF for two main reasons. First, the NAFF method seems more appropriate to extend the domain of validity of theorem 1 by continuing invariant quasi-periodic curves to larger values of T. For example, using the maximal Lyapunov exponent we cannot access the frequency of an invariant curve and, moreover, the additional information needed to locate and track invariant curves has to be obtained using other methods. Second, the numerical results we expose in section 3.3 are aimed to show that the *qualitative* presentation of the dynamics of the stirred fluid contained in the original paper by Aref [1] can be translated into a *quantitative* one. Therefore, we were not concerned with requirements of optimality, neither in the CPU time consumed nor in the accuracy of the fine structures observed.

We believe that once our preliminary research has been done, one could try to refine the numerical results illustrated here by using one of the previously cited methods. For instance, the MEGNO method seems to be more powerful to explore 'highly' chaotic domains.

2. Existence of invariant curves

In order to establish the existence of invariant curves for system (1) with the piecewise constant protocol (3) and small T, we will show that its T-Poincaré operator (i.e., its period map) satisfies the assumptions of Moser's small twist theorem.

Before outlining the strategy of our proof, for the sake of completeness it is worth recalling this result.

Fixing $I_1 > I_0 > 0$, let us consider the annulus defined by $A = \{(\bar{\theta}, I) : \bar{\theta} \in \mathbb{S}^1, I_0 \leqslant I \leqslant I_1\}$. Given a map $M : A \to \mathbb{R}^2$, we can find a lift of it to the universal cover $\mathcal{A} = \{(\theta, I) : \theta \in \mathbb{R}, I_0 \leqslant I \leqslant I_1\}$ of A, which we still denote by M.

Moser's small twist theorem. *Let α be a $C^4([I_0, I_1])$ function satisfying*

$$\alpha'(I) < 0 \qquad \forall I \in [I_0, I_1]. \tag{4}$$

Then, there exists $\epsilon > 0$, depending on $I_1 - I_0$ and α, such that the map $M : A \mapsto \mathbb{R}^2$ has invariant curves provided the following conditions are satisfied:

(a) M has the intersection property, that is, for any Jordan curve γ homotopic to the circle $I = I_0$ in A, $M(\gamma) \cap \gamma \not\equiv \emptyset$;

(b) the lift of M can be expressed in the form

$$M(\theta, I) = (\theta + T\alpha(I) + T\phi_1(\theta, I, T), I + T\phi_2(\theta, I, T)), \tag{5}$$

for some $T \in (0, 1)$ *and* $\phi_1, \phi_2 \in C^4(\mathcal{A})$ *with* $\|\phi_1\|_{C^4(\mathcal{A})} + \|\phi_2\|_{C^4(\mathcal{A})} < \epsilon$.

This version of the theorem is presented in [17] and may be proved using the techniques developed in [10, 11]. In what follows, a map of the form $(\theta + T\alpha(I), I)$ with $\alpha'(I) \neq 0$, $I \in [I_0, I_1]$, will be referred to as *small twist map*, as its twist becomes small when the parameter gets small. This is the reason why we could not use the classical Moser's twist theorem.

The previous theorem will be applied once some preliminary steps have been done; first, in section 2.1, by using a classical construction from averaging theory, we will rewrite system (1) as a 1-periodic perturbation of the Hamiltonian averaged system, with T being the small parameter. The averaged system corresponds to the two fixed agitators model. Then, exploiting the geometry of the phase space of the averaged system, we will construct explicitly the corresponding action–angle variables on a suitable subset of D_R. As a consequence, we will be able to show that on an appropriate annulus inside D_R the 1-Poincaré map of the averaged system is a small twist map.

Next, the C^4 estimates needed to apply the small twist theorem will be provided by a general result about the differentiability of a flow with respect to parameters (proposition 2 section 2.2).

Finally, in section 2.3, we collect all these intermediate steps and we complete the proof of our main theorem.

2.1. The averaged system

In what follows, we identify $\mathbb{C}$ with $\mathbb{R}^2$ and $\zeta = x + \mathrm{i}y$ with (x, y). We rewrite the Hamilton equations of system (1) in a compact real form as

$$\dot{\zeta} = J\nabla_\zeta H(t, \zeta), \tag{6}$$

where J is the standard 2×2 symplectic matrix and $\nabla_\zeta = \left(\frac{\partial}{\partial x}, \frac{\partial}{\partial y}\right)$.

The Hamilton function $H(t, \zeta)$ is piecewise autonomous and may be expressed in the form

$$H(t, \zeta) = \phi(t)H_+(\zeta) + (1 - \phi(t))H_-(\zeta),$$

where

$$H_\pm(\zeta) = \frac{\Gamma}{2\pi} \ln \left| \frac{\zeta \mp b}{b\zeta \mp R^2} \right|, \tag{7}$$

and $\phi(t)$ is the T-periodic extension of the restriction to $[0, T]$ of the characteristic function of $[0, T/2]$. Hence, defining $\mathcal{D} := \mathbb{R}^2 \backslash \{\pm b, \pm R^2/b\}$, $H(t, \zeta)$ is smooth on the set $(\mathbb{R}\backslash\{kT/2, k \in \mathbb{Z}\}) \times \mathcal{D}$. Moreover, H and its derivatives with respect to ζ, which exist in $\mathcal{D}$ for any $t \in \mathbb{R}$, have jump discontinuities at $t = kT/2, k \in \mathbb{Z}$.

The next step is to consider T as a small parameter and to determine a suitable comparison limit system when $T \to 0$. With this aim, as done in [1], we first rescale time in (6) by setting $t = T\tau$, so normalizing to 1 the period of the stirring protocol and of the vector field. In the new time τ, setting $H_1(\zeta, \tau) := H(\zeta, \tau T)$ and $y(\tau) := \zeta(\tau T)$, system (6) takes the form

$$\dot{y}(\tau) = TJ\nabla_y H_1(\tau, y). \tag{8}$$

Next, we apply averaging theory to this system (see, for instance, section 4.4 [9]). Denote

$$\hat{H}_1(y) := \int_0^1 H_1(\tau, y)\, \mathrm{d}\tau = \frac{\Gamma}{4\pi} \ln \left| \frac{y^2 - b^2}{y^2 - R^4/b^2} \right| \tag{9}$$

and let $V \subset \mathbb{C}$ be an open set such that its closure is contained in D. Then, for small enough $T_0 > 0$ we can find a symplectic[3], close to identity, change of coordinates of the form

$$y = \eta + T w(\tau, \eta), \qquad (\tau, \eta, T) \in \mathbb{R} \times V \times (0, T_0], \tag{10}$$

with w 1-periodic in τ and such that

$$w(0, \eta) = 0, \tag{11}$$

which transforms system (8) into

$$\dot{\eta} = T J \nabla_\eta \hat{H}_1(\eta) + T^2 h(\tau, \eta, T). \tag{12}$$

By construction, the function $h(\tau, \eta, T)$ in (12) is 1-periodic in τ, has jump discontinuities at $\tau = k/2, k \in \mathbb{Z}$, and is smooth on $(\mathbb{R}\backslash\{k/2, k \in \mathbb{Z}\}) \times V \times [0, T_0]$.

System (8) can be considered as a perturbation of the following (integrable) *averaged system*:

$$\dot{\eta} = T J \nabla_\eta \hat{H}_1(\eta). \tag{13}$$

Henceforth, for simplicity, we will write $\hat{H}$ instead of $\hat{H}_1$. We note that the Hamilton function $\hat{H}$ corresponds to a two point vortices system, one vortex being located at $(+b, 0)$ and the second at $(-b, 0)$. Moreover, exploiting the geometry of the phase space of system (13), we can construct explicitly the action variable for this system outside the homoclinic loops surrounding the vortices (see figure 1 (left) for $T = 0.05$). This is done as follows.

By introducing symplectic polar coordinates $\zeta = \sqrt{2r}\, \mathrm{e}^{\mathrm{i}\psi}$ and setting for notational convenience $E = \mathrm{e}^{4\pi \hat{H}/\Gamma}$, we can express the level lines of $\hat{H}$ outside the homoclinic loops

$$r(\psi) = \frac{b^2 R^4}{R^4 + b^4} \cos 2\psi, \qquad \psi \in \left[-\frac{1}{4}\pi, \frac{1}{4}\pi\right] \cup \left[\frac{3}{4}\pi, \frac{5}{4}\pi\right], \tag{14}$$

in the form $r = r(\psi, E)$ with $\psi \in \mathbb{R}$ and $E \in (b^2/R^4, 1/R^2]$. We observe that $E = 1/R^2$ corresponds to the boundary of D_R, whereas b^2/R^4 corresponds to the homoclinic loops.

Taking into account that $r(\psi, E) = r(-\psi, E) = r(\pi - \psi, E)$ (namely the averaged system is invariant with respect to $\zeta \to \bar{\zeta}$ and $\zeta \to -\bar{\zeta}$), the action variable I is given by

$$I(E) = \frac{1}{2\pi} \int_{\hat{H}(\sqrt{2r}\, \mathrm{e}^{\mathrm{i}\psi}) = \frac{\Gamma}{4\pi} \ln E} r \, \mathrm{d}\psi = \frac{a(E)}{2\pi} \int_0^{\pi/2} \sqrt{b(E) \cos^2(2\psi) + c(E)}\, \mathrm{d}\psi, \tag{15}$$

where

$$a(E) := \frac{1}{1 - E^2 b^4}, \qquad b(E) := 4b^4 (1 - E^2 R^4)^2$$
$$c(E) := 4(E^2 b^4 - 1)(b^4 - E^2 R^8).$$

In the next proposition, the explicit form of the action–angle variables constructed above will be used to show that the 1-Poincaré operator of the averaged system, denoted by $\hat{M}_1^T$, is a small twist map on an appropriate annular region inside D_R.

Proposition 1. *The set*

$$\mathcal{E} := \left\{ E \in \left(\frac{b^2}{R^4}, \frac{1}{R^2} \right] : I'(E) \neq 0 \text{ and } E I''(E) + I'(E) \neq 0 \right\},$$

[3] Introducing canonical variables $y = (p, q)$ and $\eta = (P, Q)$ the required transformation can be obtained through the following generating function $S(q, P, \tau) = Pq + T \int_0^\tau [\hat{H}_1(P, q) - H_1(P, q, s)]\, \mathrm{d}s$. Thus $p = \partial_q S$ can be inverted if T is small enough and trivially $S(q, P, \tau + 1) = S(q, P, \tau)$ for all (q, P, τ) which implies (11).

is a non-empty interval. Fix $E_0 \in (\inf \mathcal{E}, \frac{1}{R^2})$ *and consider the annulus*

$$A := \left\{ \zeta \in D_R : \frac{\Gamma}{4\pi} \ln E_0 \leqslant \hat{H}(\zeta) \leqslant \frac{\Gamma}{4\pi} \ln \frac{1}{R^2} \right\}. \tag{16}$$

Then, $\hat{M}_1^T$ *is a small twist map in A.*

Proof. An easy computation shows that $1/R^2 \in \mathcal{E}$. The remaining claims about $\mathcal{E}$ follow from the continuity of the maps $E \mapsto I'(E)$, $E \mapsto EI''(E) + I'(E)$. Let us consider action–angle coordinates (θ, I) for the averaged Hamiltonian system (13), with I given by (15). In the annular domain A defined by (16), the map $I = I(\hat{H}) := I(E(\hat{H}))$ has an inverse $\hat{H} = \hat{H}(I)$, well defined on the interval $[I_0, R^2/2]$, where $I_0 := I(E_0)$. Moreover, on such interval we have $\hat{H}''(I) \neq 0$. Since, $\hat{H}''(1/R^2) < 0$, it follows that

$$\hat{H}''(I) < 0, \qquad I \in [I_0, R^2/2]. \tag{17}$$

The 1-Poincaré map associated with system (13) admits a lift to the set $\mathcal{A} := \mathbb{R} \times [I_0, R^2/2]$ given by $\hat{M}_1^T(\theta, I) = (\theta + T\hat{H}'(I), I)$ and therefore, taking also into account (17), it follows that it is a small twist map. □

In order to apply Moser's small twist theorem, we need some further estimates. These estimates will be provided in the next section using a result which follows from the general theory of ODEs.

2.2. *Differentiability with respect to parameters*

Let $T > 0$ be the period of the stirring protocol (3) and let M_1^T be the 1-Poincaré operator of system (12). In this subsection, we state a general result, namely proposition 2, which is an immediate consequence of the differentiability of the flow of a system of ODEs with respect to parameters. This result is a restatement of proposition 6.4 in [17] under the standard assumptions considered when dealing with non-autonomous vector fields which are discontinuous in the time variable.

Proposition 2 will provide the estimates needed to show that for sufficiently small T the maps M_1^T and $\hat{M}_1^T$ are C^4-close on the annulus A defined by (16). This will be done in the next subsection, from which the proof of our main result will follow easily.

Let V be an open subset of $\mathbb{R}^n$, let T_0 be a fixed positive number, and let m be a non-negative integer. Consider the following differential equation depending on the parameter T

$$\frac{\mathrm{d}x}{\mathrm{d}t} = F(t, x, T), \tag{18}$$

where the map $F : [0, 1] \times V \times [0, T_0] \to \mathbb{R}^n$, $(t, x, T) \mapsto F(t, x, T)$ satisfies the properties below:

- the map $(x, T) \mapsto F(t, x, T)$ belongs to $C^{m+1}(V \times [0, T_0])$ for almost all $t \in [0, 1]$;
- for $0 \leqslant j + k \leqslant m + 1$, the maps $t \mapsto \frac{\partial^{k+j}}{\partial x^k \partial T^j} F(t, x, T)$ are t measurable for any $(x, T) \in V \times [0, T_0]$;
- for each compact set $K \subset V$ there exists $C > 0$ such that

$$\left| \frac{\partial^{k+j}}{\partial x^k \partial T^j} F(t, x, T) \right| \leqslant C,$$

for all $0 \leqslant k + j \leqslant m + 1$ and $(t, x, T) \in [0, 1] \times K \times [0, T_0]$.

The solution of (18) satisfying $x(0) = x_0$ will be denoted by $x(t; x_0, T)$. By the general theory of ordinary differential equations, x is of class $C^{0,m+1,m+1}$ in its three arguments whenever it is defined. The following result is a consequence of this fact.

Proposition 2. *Let A be a compact subset of V such that for every $x_0 \in A$ and $T \in [0, T_0]$ the solution $x(t; x_0, T)$ is well defined in $[0, 1]$. Then, for each $(t, x_0, T) \in [0, 1] \times A \times [0, T_0]$ the expansion below holds*

$$x(t; x_0, T) = x(t; x_0, 0) + \frac{\partial x}{\partial T}(t; x_0, 0)T + R(t; x_0, T)T,$$

where the remainder R satisfies

$$\|R(t; \cdot, T)\|_{C^m(A)} \to 0, \qquad T \to 0,$$

uniformly in $t \in [0, 1]$.

2.3. Proof of theorem 1

We are now able to prove our main theorem. We will show that for sufficiently small T the T-Poincaré map associated with system (1) with the stirring protocol (3) has invariant curves in the set A defined by (16).

For a fixed R' satisfying $R < R' < R^2/b$, we define

$$V := \left\{ \zeta = \sqrt{2r}\, \mathrm{e}^{\mathrm{i}\psi} \in \mathbb{C} : \frac{b^2 R^4}{R^4 + b^4} \cos 2\psi < r < (R')^2/2 \right\}. \tag{19}$$

This set, which contains A, corresponds to the open disc of radius R' minus the compact region bounded by the homoclinic loops. Hence, it has positive distance from the singularities of $\hat{H}$. Now we choose a sufficiently small $T_0 > 0$ for which the transformation (10) is well defined on $[0, 1] \times V \times [0, T_0]$ and for which, moreover, all the solutions of system (8) with initial conditions in A are well defined in $[0, 1]$. Let $T < T_0$ be the period of $z(t)$. By proposition 2, and by introducing the action–angle variables considered in proposition 1, we can find a lift of M_1^T to $\mathcal{A} := \mathbb{R} \times [I_0, R^2/2]$ of the form

$$M_1^T(\theta, I) = (\theta + \hat{H}'(I)T, I) + R(\theta, I, T)T,$$

where $\|R(\cdot, T)\|_{C^4(\mathcal{A})} \to 0$ for $T \to 0$. Hence, M_1^T satisfies hypothesis (b) of Moser's small twist theorem for T small enough. Moreover, M_1^T has the intersection property in A, being an area-preserving map in A for which the outer boundary of A is invariant.

Then, by Moser's small twist theorem, M_1^T has many invariant curves in A for T small enough, and so does the T-Poincaré operator of system (1), which obviously coincides with M_1^T.

3. Numerical results

In this section, we will study system (1) with the stirring protocol (3) from a numerical point of view. More precisely, we will be interested in two types of numerical experiments. In the first one, we will explore the *continuation* properties with respect to T of the invariant curves of the T-Poincaré map of system (1) obtained for small T with theorem 1. In section 3.2, we will give numerical evidence of their persistence close to the boundary up to (some) large values of T.

In the second experiment, we will be able to give a *quantitative* description of the mixing efficiency of the piecewise constant stirring protocol varying the parameters (b, T).

Both these numerical experiments will be carried out by using the numerical analysis of the fundamental frequency (NAFF) of Laskar [13].

This is a numerical method which allows one to obtain a global view of the behaviour of a dynamical system by studying the properties of the frequency map, numerically defined from the action-like variables to the frequency space using adapted Fourier techniques. This method has been used to investigate a wide class of dynamical systems, such as the solar system [14], the galactic dynamics [18], particle accelerators [15] and the standard map [3].

For the sake of completeness, we briefly present the outlines of the method, referring to [13] for further details, and we postpone our results to the next section.

3.1. Frequency map analysis

Let us consider an n-degrees of freedom quasi-integrable Hamiltonian system, expressed in action–angle variables by

$$H(I, \theta; \epsilon) = H_0(I) + \epsilon H_1(I, \theta), \tag{20}$$

where H is a real analytic function of $(I, \theta) \in B \times \mathbb{T}^n$, B is an open domain in $\mathbb{R}^n$, $\mathbb{T}^n$ is the n-dimensional torus, and ϵ is a small real parameter. For $\epsilon = 0$ the system is integrable: the motion takes place on invariant tori $I_j = I_j(0)$ described at constant velocity $\nu_j(I) = \frac{\partial H_0}{\partial I_j}\big|_{I(0)}$, for $j = 1, \ldots, n$. Assuming a non-degeneration condition on H_0, the frequency map $F : B \to \mathbb{R}^n$

$$F : I \mapsto F(I) = \nu,$$

is a diffeomorphism onto its image Ω. In this case, KAM theory [12, 2, 16] ensures that for sufficiently small values of $|\epsilon|$, there exists a Cantor set $\Omega_\epsilon \subset \Omega$ of frequency vectors satisfying a Diophantine condition, for which the quasi-integrable system with Hamilton function (20) still possesses smooth invariant tori. These tori are ϵ-close to those of the unperturbed system, and support the linear flow $t \mapsto \theta_j(t) = \nu_j t + \theta_j(0) (\mathrm{mod}\, 2\pi)$ for $j = 1, \ldots, n$. Moreover, according to Pöschel [19] there exists a diffeomorphism $\Psi : \mathbb{T}^n \times \Omega \to \mathbb{T}^n \times B$,

$$\Psi : (\phi, \nu) \mapsto (\theta, I),$$

which is analytic with respect to ϕ in $\mathbb{T}^n$ and $\mathcal{C}^\infty$ w.r.t. ν in Ω_ϵ, and which transforms the Hamiltonian system generated by (20) into

$$\begin{cases} \dfrac{\mathrm{d}\nu_j}{\mathrm{d}t}(t) = 0 \\ \dfrac{\mathrm{d}\phi_j}{\mathrm{d}t}(t) = \nu_j. \end{cases}$$

For frequency vectors $\nu \in \Omega_\epsilon$, the invariant torus can be represented in the complex variables $(z_j = I_j \, \mathrm{e}^{\mathrm{i}\theta_j})_{j=1,n}$ by a quasi-periodic function

$$z_j(t) = z_j(0) \, \mathrm{e}^{\mathrm{i}\nu_j t} + \sum_m a_{j,m}(\nu) \, \mathrm{e}^{\mathrm{i}\langle m, \nu \rangle t}. \tag{21}$$

Taking a section $\theta = \theta_0$ of the phase space, for some $\theta_0 \in \mathbb{T}^n$, we obtain the frequency map $F_{\theta_0} : B \to \Omega$,

$$F_{\theta_0} : I \mapsto \pi_2(\Psi^{-1}(\theta_0, I)), \tag{22}$$

where $\pi_2(\phi, \nu) = \nu$ is the projection onto Ω. For sufficiently small $|\epsilon|$ the non-degeneration condition ensures that F_{θ_0} is a smooth diffeomorphism.

If we have a numerical (complex) signal over a finite time span $[-K, K]$ and we want to recover a quasi-periodic structure, we can construct an N-terms quasi-periodic approximation

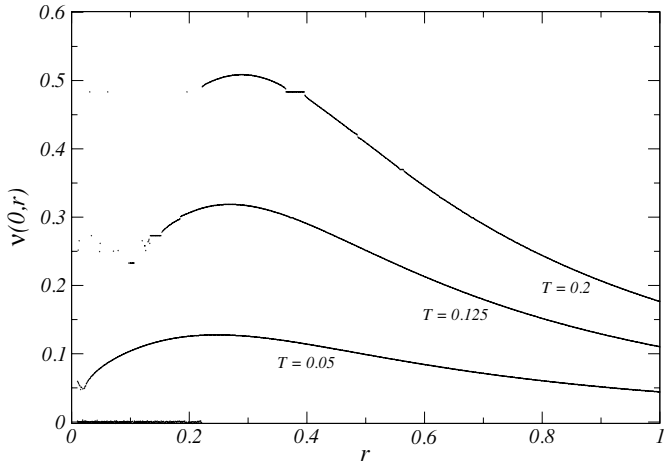

Figure 2. The frequency map numerically reconstructed by NAFF. Parameters are $b = 1/2$, $R = 1$ and $T \in \{0.05, 0.125, 0.2\}$. Initial data are 1000 points $\zeta_j(0) = \mathrm{i}r_j$, equally spaced on [0, i], and orbits are computed for $N_{\mathrm{iter}} = 50\,000$.

$\hat{f}(t) = \sum_{k=1}^{N} a_k^{(K)} \mathrm{e}^{\mathrm{i}t\nu_k^{(K)}}$. Frequencies $\nu_k^{(K)}$ and amplitudes $a_k^{(K)}$ are determined with an iterative scheme (possibly) involving some weight function (Hanning filter).

Assuming some 'good' arithmetic properties of the frequencies and using the pth Hanning filter, one can prove [13] that NAFF converges towards the first[4] 'true' frequency of the given signal, ν_1, with the following asymptotic expression for $K \to +\infty$,

$$\left|\nu_1 - \nu_1^{(K)}\right| = \mathcal{O}\left(\frac{1}{K^{2p+2}}\right), \tag{23}$$

which will usually be several orders of magnitude better than the $\mathcal{O}(1/K)$ order obtained with FFT.

Using the NAFF algorithm, it is possible to construct numerically a frequency map (see figure 2) in the following way:

(a) fix all angles to some value θ_0;
(b) for all initial values I_0 of the action variables, integrate numerically the trajectories with initial condition (I_0, θ_0) over the time span K;
(c) look for a quasi-periodic approximation of the trajectory, with the previous algorithm identifying the fundamental frequency $\nu_1^{(K)}$ of this quasi-periodic approximation.

Because of (23), we can use the NAFF algorithm to test the goodness of the reconstructed quasi-periodic approximation of the given signal[5], eventually showing numerical evidence that motion does not take place on invariant tori because of some 'diffusion in frequency space'. More precisely, this can be accomplished by replacing step (c) of the previous algorithm with the following:

(c′) divide the time span $[-K, K]$ into smaller parts (possibly overlapping): $[t_l, t_l + K_1]$, for some $(t_l)_l$. Then NAFF reconstructs for each l a frequency $\nu^{(K_1)}(l)$. If the frequencies $(\nu^{(K_1)}(l))_l$ coincide, up to some prescribed numerical precision, when l varies, then we

[4] We assume that frequencies are enumerated according to decreasing amplitudes: $\left|a_k^{(K)}\right| \geqslant \left|a_{k+1}^{(K)}\right|$; that is, some smoothness of the signal is assumed.

[5] A similar strategy has been proposed and used in [8], section 6.2, p 42.

can conclude that we obtained a good quasi-periodic approximation. Otherwise, we can measure the diffusion in the frequency space.

3.2. Application I: existence of invariant curves

Let us consider the problem of the existence of invariant curves homotopic to the boundary of D_R for the T-Poincaré map of system (1) with stirring protocol (3). One readily realizes that every such curve will intersect the vertical segment $\ell := \{\zeta \in \mathbb{C} : x = 0, y \in [0, R]\}$.

In order to reconstruct a frequency map, we fix a piecewise constant stirring protocol by choosing the parameters (b, T). Then, for N initial data on the segment ℓ we construct numerically the T-Poincaré map and we iterate it N_{iter} times.

Remark 1 (numerical computation of the Poincaré map)**.** As already remarked in [1], one can construct the Poincaré map for the piecewise constant protocol avoiding the integration of the Hamiltonian system (1), which consumes much CPU time and introduces additional errors. The idea is that in each half-period the Hamiltonian system is autonomous, hence integrable and, moreover, the integration can be explicitly done: for $t \in [0, T/2)$, the motion takes place on an arc of circle with radius $\rho = \frac{\lambda}{1-\lambda^2}\left(\frac{R^2}{b} - b\right)$, centred at $\zeta_c = \frac{b^2-\lambda^2R^2}{b(1-\lambda^2)}$, with $\lambda = b\left|\frac{\zeta(0)-b}{b\zeta(0)-R^2}\right|$. Thus, setting $\zeta(0) = \zeta_c + \rho\, \mathrm{e}^{\mathrm{i}\phi(0)}$, after half-period the point will be at $\zeta(T/2) = \zeta_c + \rho\, \mathrm{e}^{\mathrm{i}\phi(T/2)}$ where

$$\phi(T/2) - \frac{2\lambda}{1+\lambda^2}\sin\phi(T/2) = \frac{\Gamma}{2\pi\rho^2}\frac{1-\lambda^2}{1+\lambda^2}\frac{T}{2}. \tag{24}$$

The motion in the second half-period is similar.

Equation (24) can be solved using a sixth-order Newton's-type method. However, when b is close to R and/or T is large, Newton's algorithm does not converge to the good solution unless we provide a very accurate approximation of $\phi(T/2)$ as an initial value for the algorithm. In order to overcome this difficulty we used the following trick. Equation (24) is nothing but *Kepler's equation* and in [21] an explicit solution is given in terms of Bessel's functions (which turns out to be computationally less efficient than our Newton's-type method). Nevertheless, for large values of the parameters we obtain a good approximation to start with Newton's algorithm by summing few terms of the previous explicit solution.

Once we have an orbit, $\left(M_T^k(\zeta(0))\right)_{0\leqslant k\leqslant N_{\text{iter}}}$, we use the NAFF algorithm to reconstruct a quasi-periodic approximation of it. The frequency map is not smooth at all because of the presence of resonances: there is no invariant curve with a rational rotation number, namely the periodic point of M_T. Thus, for a fixed resolution, the existence of invariant curves is *assumed* if the frequency map looks 'regular' (see figure 2 for $T = 0.05$), whereas with 'irregular' graphs we associate non-existence of invariant curves (see figure 3 for $T \in \{0.5, 1.0, 1.5\}$). This first analysis can be made more rigorous, when necessary, by measuring the oscillation of the frequency curve and/or the strength of its first derivative, and we decide to call a frequency curve irregular if this measure is above some threshold value (this kind of analysis has been used in [3]).

In figure 2 we present some numerical results for the piecewise constant protocol (3) with $b = 1/2$ and several values of T. For very small T, say 0.05, the curve looks regular, hence a large part of the disc is occupied by invariant curves. We can observe that the map *is not twist* in the whole disc: there is a point where the derivative of the frequency map is zero. For slightly larger T, say $T \in [0.125, 0.2]$, the curve is still regular, but an irregular pattern is showed close to the origin. Roughly speaking, no invariant curves are present for $T = 0.2$

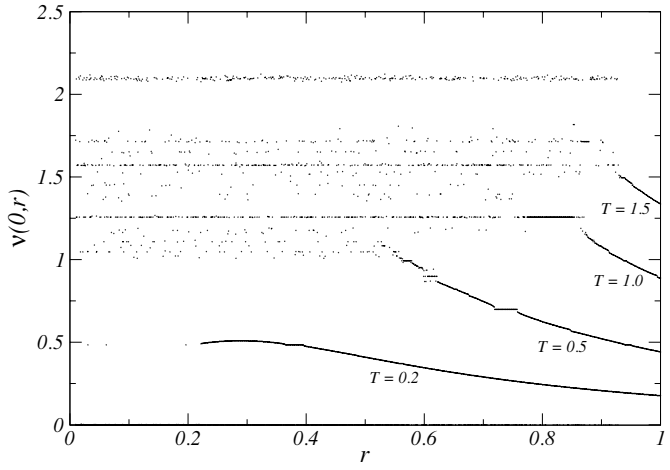

Figure 3. The frequency map numerically reconstructed by NAFF. Parameters are $b = 1/2$, $R = 1$ and $T \in \{0.2, 0.5, 1.0, 1.5\}$. Initial data are 1000 points $\zeta_j(0) = \mathrm{i}r_j$, equally spaced on [0, i], and orbits are computed for $N_{\mathrm{iter}} = 50\,000$.

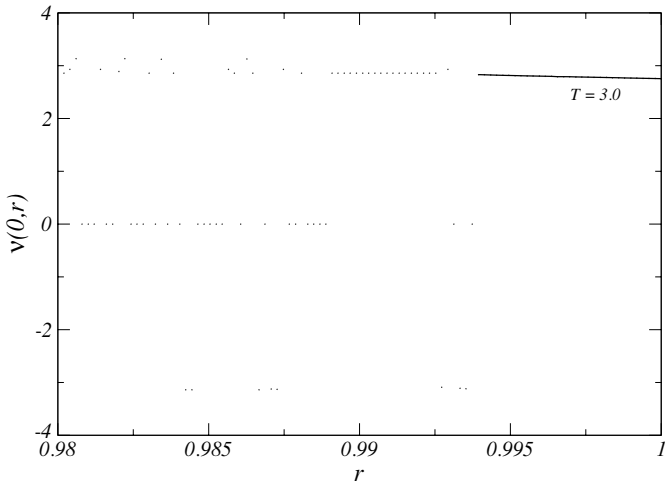

Figure 4. The frequency map numerically reconstructed by NAFF. Parameters are $b = 1/2$, $R = 1$ and $T = 3.0$. Initial data are 1000 points $\zeta_j(0) = \mathrm{i}r_j$, equally spaced on [0.98i, i], and orbits are computed for $N_{\mathrm{iter}} = 500\,000$.

in the disc $|\zeta| \leqslant 0.22$ and in the disc $|\zeta| \leqslant 0.16$ for $T = 0.125$. Also, elliptic points due to resonances are shown (horizontal plateaux).

In figure 3, as T increases, the irregular patterns consume larger and larger portions of the invariant disc, but still a regular frequency curve is present close to the boundary of D_R.

This behaviour is emphasized in figure 4, where we show a numerical result for $b = 1/2$ and $T = 3.0$, a period which is 60 times larger than the smallest value in figure 2. Note the change of horizontal scales between figures 2 and 3 (the scale on the vertical axis has also been changed to show the large oscillations of the frequency curve).

Other results for larger values of T exhibit a similar behaviour. This supports the conjecture that invariant curves persist, close to the boundary, for arbitrarily large values of T.

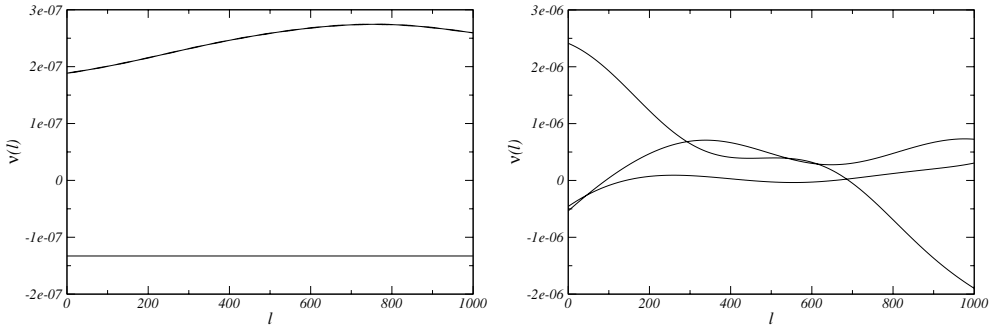

Figure 5. Distance between the frequency $\nu_1^{(K_1)}(l)$, determined by NAFF, and the mean value of the $\nu_1^{(K_1)}(l)$, as a function of the part of orbit $[t_l, t_l + K_1]$. Left: very regular orbits; right: less regular ones (compare vertical scales). Both plots are made with $N_{\text{iter}} = 100\,000$, $K_1 = 50\,000$ and $t_l = 50(l-1)$.

3.3. Application II: mixing efficiency

We have already observed that invariant curves are an obstruction to global mixing. We remark now that close to *robust* invariant curves (i.e., associated with 'good' frequencies) there is a neighbourhood filled by invariant curves [6, 7], which also prevents local mixing. Using the precision of the result we could obtain using NAFF and observation (c′), we can test the efficiency of the stirring protocol by evaluating the goodness of the reconstructed signal.

More precisely, we fix a couple of parameters (b, T), then we divide the invariant disc D_R into a fine grid of N_{tot} points. For each point we determine numerically (see remark 3.2) the orbit for a time interval $[0, K]$. Then, fixing some $K_1 < K$ and some positive $(t_l)_l$ we divide the orbit into pieces $(\zeta(t))_{t\in[t_l,t_l+K_1]}$, such that intervals $[t_l, t_l + K_1]$ overlap. On each piece, the use of NAFF gives us a fundamental frequency $\nu^{(K_1)}(l)$, where we emphasized the dependence of the frequency on the lth piece of the orbit.

Hence, for a given orbit with initial datum $\zeta_0 = (x_0, y_0)$, we define

$$\varepsilon(x_0, y_0) = -\log\left|2\,\frac{\max_l \nu^{(K_1)}(l) - \min_l \nu^{(K_1)}(l)}{\max_l \nu^{(K_1)}(l) + \min_l \nu^{(K_1)}(l)}\right|. \tag{25}$$

This is a good indicator of the robustness of the orbit. In fact, if $\varepsilon(x_0, y_0)$ is 'large' then $\max_l \nu^{(K_1)}(l)$ and $\min_l \nu^{(K_1)}(l)$ are 'close together'. Thus, the reconstructed frequencies on different pieces of the orbit do not vary too much, and we can assume that we are on a quasi-periodic orbit. On the other hand, if $\varepsilon(x_0, y_0)$ is 'small' then $\max_l \nu^{(K_1)}(l)$ and $\min_l \nu^{(K_1)}(l)$ are 'far from each other'. In this case, since the reconstructed frequency is not constant, we conclude that we are not on a quasi-periodic orbit. Intermediate values of $\varepsilon(x_0, y_0)$ give rise to intermediate degrees of robustness. Existence of invariant curves is an obstruction to mixing and thus affect global mixing efficiency; close to a robust curve also local mixing is poor because of the 'large number' of barriers.

We now fix a threshold value $\varepsilon_{\text{thr}} > 0$ and we measure the portion of initial data in D_R with which one can associate a ε_{thr}-robust orbit

$$m_{\varepsilon_{\text{thr}}} = \frac{\#\{(x_0, y_0) : \varepsilon(x_0, y_0) > \varepsilon_{\text{thr}}\}}{\#\{(x_0, y_0)\}}. \tag{26}$$

A preliminary analysis, see figure 5, of the robustness of some typical orbits, allows us to choose an appropriate threshold value.

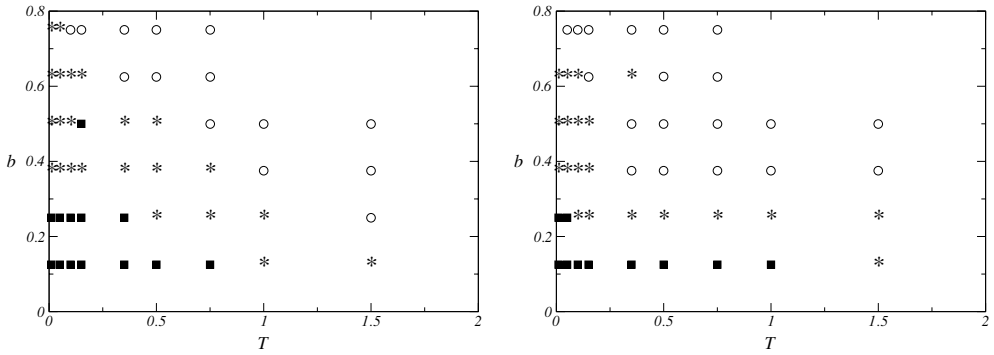

Figure 6. A part of parameter plane and the corresponding $m_{\varepsilon_{\text{thr}}}$ function; left: m_{12}; right: m_{15}. 'Squares' correspond to the integrable case (I), 'stars' to the transitional (T) and 'circles' to the chaotic (C).

In this way, we are able to turn the *qualitative* analysis of figure 7, p 738, of [1] into a *quantitative* one.

We present two results, the first with $\varepsilon_{\text{thr}} = 12$, corresponding to $\left|\frac{\max_l \nu^{(T_1)}(l)}{\min_l \nu^{(T_1)}(l)} - 1\right| \leqslant 310^{-6}$, and the second with $\varepsilon_{\text{thr}} = 15$ and $\left|\frac{\max_l \nu^{(T_1)}(l)}{\min_l \nu^{(T_1)}(l)} - 1\right| \leqslant 1.510^{-7}$. Each result has been obtained dividing the invariant disc in approximately 30 000 points, equally spaced in both x and y by 0.01. Then, several values of b and T have been considered.

Finally, by using the previous ideas, we make precise the classification scheme given for a regime at p 736 of [1] as follows:

[**I**] *integrable,* if $0.6 < m_{\varepsilon_{\text{thr}}} \leqslant 1$ (very poor mixing property);
[**T**] *transitional,* if $0.3 < m_{\varepsilon_{\text{thr}}} \leqslant 0.6$;
[**C**] *chaotic,* if $0 < m_{\varepsilon_{\text{thr}}} \leqslant 0.3$ (efficient mixing).

We summarize our results in figure 6.

4. Conclusions

In this paper, we proved (in theorem 1) that the simple stirring model given by (1) with the stirring protocol (3) has invariant curves for all T small enough and every $b \in [0, R)$; the use of NAFF gives us numerical evidence that such invariant curves persist even for some large values of T closer and closer to the boundary of the disc as T increases. Hence, for small T the mixing efficiency in not good at all, whereas for larger values of T, say $T > 1$, it becomes reasonably good once $b \geqslant R/2$. Thus, even if very simple, the model can give rise to efficient mixing.

We point out that the proof of theorem 1 relies on general results, namely on the theory of averaging, on the smooth dependence of flows on parameters, and on Moser's small twist theorem. Thus, this setting can be used to prove results similar to theorem 1 for more general T-periodic stirring protocols $z(t)$. However, it must be emphasized that the starting point should be to obtain a 'simple' averaged system.

From the numerical point of view, systems with a more general protocol can be surely studied by means of the NAFF method, once we obtain good symplectic integrators for these systems. Still considering our piecewise constant model, we think that using NAFF one could give precise estimates of the size of the annular domain close to the boundary of D_R

containing invariant curves and of the rate at which it shrinks to zero when T increases to infinity, providing thus a quantitative interpretation of figure 8, p 738, of [1]. This kind of analysis could be certainly supported with other numerical methods adapted to 'detect the degree of chaos' in hyperbolic regimes, for instance the MEGNO [5]. However, this deserves further investigations, which will be performed in a future paper.

Acknowledgments

Support from GRICES/CNR project 2003/2004 is acknowledged. The second author was also supported by FCT. We would like to thank Professor Rafael Ortega for some very useful suggestions.

References

[1] Aref H 1984 Stirring by chaotic advection *J. Fluid Mech.* **143** 725–45
[2] Arnold V I 1963 Proof of a theorem of A N Kolmogorov on the invariance of quasiperiodic motions under small perturbations of the Hamiltonian *Usp. Mat. Nauk.* **18** 13
Arnold V I 1963 *Russ. Math. Surv.* **18** 9–36
[3] Carletti T and Laskar J 2000 Scaling law in the standard map critical function, interpolating Hamiltonian and frequency analysis *Nonlinearity* **13** 1–29
[4] Cincotta P M and Simó C 2000 Simple tools to study global dynamics in non-axisymmetric galactic potentials—I *Astron. Astrophys. Suppl. Ser.* **147** 205–28
[5] Cincotta P M, Giordano C M and Simó C 2003 Phase space structure of multi-dimensional systems by means of the mean exponential growth factor of nearby orbits *Physica* D **182** 151–78
[6] Giorgilli A and Morbidelli A 1995 Superexponential stability of KAM tori *J. Stat. Phys.* **78** 1607–17
[7] Giorgilli A and Morbidelli A 1995 On a connection between KAM and Nekhoroshev's theorems *Physica* D **86** 514–6
[8] Gómez G, Mondelo J M and Simó C Refined Fourier analysis: procedures, errors estimates and applications *Preprint Barcelona UB-UPC Dynamical Systems Group* Num 31.2001, http://www.maia.ub.es/dsg/2001/
[9] Guckenheimer J and Holmes P 1983 Nonlinear oscillations, dynamical systems, and bifurcation of vector fields *Appl. Math. Sci.* **42**
[10] Herman M R 1983 Sur les courbes invariantes par les difféomorphismes de l'anneau I *Asterisque* I **103-104**
[11] Herman M R 1986 Sur les courbes invariantes par les difféomorphismes de l'anneau I *Asterisque* II **144**
[12] Kolmogorov A N 1954 Preservation of conditionally periodic movements with small change in the Hamilton function *Dokl. Akad. Nauk SSSR* **98** 527–30
[13] Laskar J 1999 Introduction to frequency map analysis *Proc. 3DHAM95 NATO Advanced Institute 533 (S'Agaro, June 1995)* pp 134–50
[14] Laskar J 1990 The chaotic motion of the solar system. A numerical estimate of the size of the chaotic zones *Icarus* **88** 266–91
[15] Laskar J and Robin D 1996 Application of frequency map analysis to the ALS *Part. Accel.* **54** 183–92
[16] Moser J K 1962 On invariant curves of area preserving mappings of an annulus *Nachr. Akad.: Wiss. Gottingen Math. Phys.* II 1–20
[17] Ortega R 2000 Twist mappings Invariant curves and periodic differential equations *Prog. Nonlinear Diff. Eqns Appl.* **43** 85–112
[18] Papaphilippou Y and Laskar J 1996 Frequency map analysis and global dynamics in a two degrees of freedom galactic potential *Astron. Astrophys.* **307** 427–49
[19] Pöschel J 1982 Integrability of hamiltonian systems on cantor sets *Commun. Pure Appl. Math.* **25** 653–95
[20] Simó C 2005 On the use of Lyapunov exponent to detect global properties of the dynamics *Proc. Equadiff 2003* (Singapore: World Scientific)
[21] Watson G N 1966 *A Treatise on the Theory of Bessel Functions* 2nd edn (Cambridge: Cambridge University Press)